The Synthetic Aperture Mapping Sonar SAMS150 onboard UlyX AUV 6000m : An advanced solution for simultaneous detection and identification of deep-sea features

Charlot D. [1], Couade M. [2], Marty B. [3], Fabre M. N. [3], Alain P. [1], Delbecke J. [1], Laquet Th. [3], Chemisky B. [3], Mosca F. [3], Bouhier Marie-Edith [4], Brignone Lorenzo [4], Jaussaud Patrick [4], Opderbecke Jan [4]

[1] Exail,System Sonar Division,Brest,France
[2] AustralDx,Paris,France
[3] Exail,System Sonar Division,La Ciotat,France
[4] Centre méditerranée, Ifremer, La Seyne sur Mer, France

Email addresses : didier.charlot@exail.com ; mcouade@australdx.fr ; baptiste.marty@exail.com ; marie.noelle.fabre@exail.com ; philippe.alain@exail.com ; jacques.delbecke@exail.com ; thomas.laquet@exail.com ; bertrand.chemisky@exail.com ; frederic.mosca@exail.com ; marie.edith.bouhier@ifremer.fr ; lorenzo.brignone@ifremer.fr ; patrick.jaussaud@ifremer.fr ; Jan.Opderbecke@ifremer.fr

Abstract :

The use of Autonomous Underwater Vehicles (AUVs) equipped with sonars has become increasingly important in oceanographic research, environmental monitoring, and industrial applications. Synthetic Aperture Sonars (SAS) have gained particular attention due to their ability to provide high-resolution three-dimensional (3D) images of the seafloor. However, the integration of SAS onto AUVs is still a significant technical challenge, as it requires the development of high reliability and robust systems. In this study, we present the technical details on the integration of an Interferometric Synthetic Aperture Sonar (SAMS-150) developed at Exail, on a new deep sea AUV "UlyX" developed by the French Research Institute for Exploitation of the Sea (Ifremer),as well as the results of a series of test missions conducted in real-world environments.

Keywords : synthetic aperture sonar, interferometry, cartography, hydrography, deep sea mapping

I. INTRODUCTION

Synthetic aperture sonar (SAS) systems, initially developed for mines detection in military applications , start to be used in civil applications. They theoretically offer the best compromise between coverage rate and along track resolution compared to single-beam or multi-beam side-scan sonar. However, hydrographic and offshore applications have specific constraints existing SAS systems do not fulfill, such as robustness to environmental and navigation conditions, precise absolute georeferencing in real-time, cost effectiveness, integrability, ease of use, and hydrographic qualification. The Synthetic Aperture <u>Mapping</u> Systems (SAMS) have been designed to address most of these constraints. Historically, the concept of the synthetic aperture mapping sonar (SAMS) system has emerged about 18 years ago with the first system developed at iXsea (now Exail) in 2006 [1] . From a system point-of view it is a strapdown integration of positioning and navigation system (USBL/INS) linked to a side-scan sonar hardware characterized by a wide

emission aperture (typically 5°) , and a multi-hydrophone linear reception array. This concept of mapping synthetic aperture sonar has evolved to include all intermediate sonar imaging techniques from multibeam real aperture side-scan , incoherent synthetic aperture to high resolution coherent synthetic aperture [2]. The latest generation of the SAMS, the SAMS150, benefits from many new features: improvement in processing algorithms and their hardware/software integration and implementation of interferometric capabilities. The first prototype of SAMS150 has been integrated into the 6000m depth rated AUV UlyX developed by Ifremer. The UlyX AUV system is an observation platform equipped with a complete set of payloads (Digital still camera, Forward looking and multibeam bathymetry sonar, echosounder, physical& chemical measurements devices) dedicated to the exploration of deep ocean resources and high-resolution mapping [4]. The paper will be organized as follows: Part 2 will be dedicated to the principles of SAS imaging and to the design and performances of the SAMS 150 system. Part 3 will focus on some important aspects of the SAMS processing algorithms. In Part 4, we will emphasize the specific vehicle integration, describing the hardware and software architecture within the AUV system. Resulting imaging performances will be illustrated and discussed on real data sets acquired during recent sea-trials. We will conclude by discussing of developments in the short and medium term.

II. SAMS150 DESIGN AND PERFORMANCES

In the first three sections, A, B, and C, we will briefly review some fundamental aspects of SAS imaging principles in both coherent and incoherent modes. In section C, we will demonstrate that the coherent SAS imaging mode is the optimal design to achieve the best tradeoff between coverage rate and resolution for speed-limited platforms.

A. SAS imaging : performances and constraints

The SAS imaging principle and algorithms are well documented [3]: the basic principle is to synthetize a long antenna array by coherently adding the signals reflected from the same resolution cell during multiple emissions. The theoretical across track resolution δ is then independent of the range and is inversely proportional to the emission aperture width θ_e.

$$\delta = \frac{\lambda}{2\theta_e} = \frac{L_e}{2} \qquad (1)$$

where L_e is the antenna emission length, λ is the central wavelength.

To achieve this imaging performance two sampling conditions at the receiver aperture must be met.

: first, the spatial real-aperture sampling condition impose that the inter-sensor distance is less than the emission length . Second, the spatial synthetic aperture sampling requires that

the displacement on between two consecutive emissions is less than half the length of the reception antenna.

These two conditions ensure that the grating lobes of the real and synthetic aperture are outside the main lobes.

$$d < L_e \quad \text{and} \quad D < L_r/2 \qquad (2)$$

In coherent imaging, the precision on the relative positions on emitter and receiver on two consecutive emissions should be a fraction of a wavelength. One of the most robust methods to reach such a precision is to estimate the fine displacement by hybridation of measurements given by an inertial navigation system (INS) and the relative displacement measured by acoustic correlation on redundant phase centers [5][6]. In fact, under conditions 2a and 2b , two adjacent sensors on the receiver antenna are correlated and two consecutive ping images are also correlated.

The gain in resolution is proportional to the number of integrated pings which is limited by the signal to noise ratio at far range. Typically, 10-20 ping integrations are performed to achieve high-resolution gain. However, to maintain a high-resolution gain, each pixel must remain inside the emission aperture during the integration time of the synthetic aperture, which imposes a limit on the yaw/pitch platform. If the platform stability is poor , the resolution gain will decrease. In harsher conditions, coherent integration is maintained by integrating fewer pings but at the cost of decrease in resolution gain.

B. Incoherent imaging : performances and constraints

In incoherent synthetic aperture imaging technique [7] , only the amplitude of the ping images is integrated over multiple emissions. The along track resolution is only slightly improved but at the same time the signal to noise ratio (SNR) is increased as $20\log_{10} N$ where N is the number of pings integrated in each resolution cell and the coherent noise ("speckle") is suppressed. The second constraint (2b) no longer exist. The precision needed in relative displacement is only driven with the pixel resolution not the fraction of the wavelength. Also, the stability constraint on platform navigation is relaxed . The incoherent imaging technique is a very robust imaging mode allowing full coverage and high image quality even in rough environmental and navigation conditions. It is, therefore, a powerful imaging technique for seabed exploration at high coverage rate (full coverage) , seabed imaging classification (no speckle) and feature detection (higher SNR).

C. Coverage rate and resolution in side-scan imaging systems

When the sonar speed is limited , the best tradeoff between area coverage rate (ACR) and resolution is achieved with coherent SAS imaging systems.

The coverage rate C_r is defined as the ratio between the insonified area A and the recurrence period $T_r = 2R/c$. The insonified area A is expressed as the product of the maximum range R and the maximum displacement D of the sonar system without creating hole in the insonified area. Hence the general formulation of the area ACR is :

$$ACR = \frac{A}{T_r} = \frac{2DR}{T_r} = Dc = 2RV_{max} \qquad (3)$$

The factor 2 accounts for port and starboard emission

We introduce the R_{min} parameter : it is the minimum range at which the sonar beam ensures a full coverage on the seabed . We denote α the ratio R/R_{min} where R is the maximum range. The coverage rate for the three imaging mode is then :

- Single beam sidescan coverage rate ACR_{sss}

In single beam sidescan , the maximum displacement is dictated by the azimuth swath width at reception $D_{sss} = R_{min} \theta_r$ where θ_r is the reception aperture ie $\theta_r = \lambda/L_r$. Defining $\delta_{sss} = \lambda R/L_r$ the along-track resolution, we get :

$$ACR_{sss} = 2RV_{max} = \alpha c \delta_{sss} \qquad (4)$$

- Multibeam or incoherent SAS coverage rate ACRisas

In incoherent SAS the maximum displacement allowed is defined by the emission aperture

$D_{isas} = R_{min} \theta_e$ where θ_e is the emission aperture ie $\theta_e = \lambda/L_e$. . Defining $\delta_{isas} = \lambda R/L_r$ the along-track resolution, we get :

$$ACR_{isas} = \alpha c \delta_{sss}(L_r/L_e) \qquad (5)$$

- Coherent SAS coverage rate ACR_{csas}

In coherent SAS , the maximum allowable displacement is half of the reception antenna length, $D_{csas} = L_r /2$. we get :

$$ACR_{csas} = 2RV_{max} = c\,(L_r/2) \qquad (6)$$

Equations (4) and (5) show that for incoherent or single beam side-scan , increasing the ACR would always degrade the along track resolution when the maximum speed is limited. In SAS coherent imaging, since the resolution and ACR are not linked (6) , a higher coverage rate can be obtained. This is illustrated in Fig. 1 below.
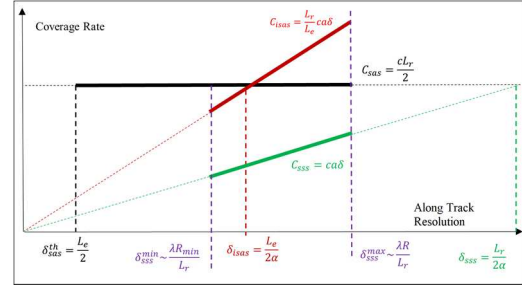

Fig. 1. : Coverage rate and resolution in Sides-scan sonar imaging systems

D. Sams150 specifications

The SAMS150 systems have been designed to meet the operational needs and constraints of an hydrographic sonar imaging system installed on an AUV or towed fish navigating near the sea bottom: the platform speed is usually 3-4 knots, the altitude above the sea bottom is a few tens of meters, and the required resolution is better than 10cm. When applying the sonar equation to SAS coherent imagery, the model predicts a 10dB signal to noise ratio at central frequency of 150khz (Fig. 2). In the model, the following parameters have been used: Source Level: SL = 218dB re.1Pa@1m, Range R = 250 m , Backscattering strength BS_0=-40dB. In fact, the 150khz central frequency is a good compromise because it provides a rather large range (about 250m) at a reasonable SAS gain of 20 at maximum range 250m.
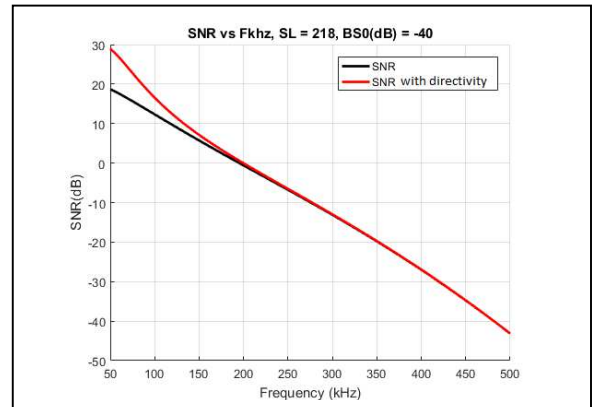
Fig. 2. : Predicted SNR vs central frequency at 250m range

After determining the central frequency, the complete design of the antennas can be computed based on the maximum range and nominal speed requirements. This includes the emitter antenna aperture and length, receiver antenna length, and number of receivers per antenna. The final specifications of the SAMS150 are shown in Table I. The SAMS 150 receiver antennas are modular and can be made of up to 3 modules, each module is being composed of an interferometric array with two superposed 60cm long linear antennas with 8 receiver channels. The SAMS150 sonar kit is shown on Fig. 3: emission antenna, reception module, electronic container, and main box.

TABLE I.   SAMS 150 SPECIFICATIONS

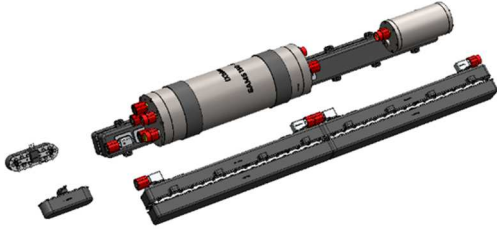| SAMS150	Specifications
Central frequency	150KHz
Maximum range	250m
Bandwidth	30KHz
Channels/side	16-32-48
Antenna length	0.6m-1.2m-1.8m
Processing	GPU
resolutions	7.0cm/2.5cm
Operating depth	Up to 6000m
Emission level	218dB (re.1Pa@1m)
Aperture width	5°x50°

Fig. 3. : SAMS150 sonar kit

III. SAMS PROCESSING

A. Introduction

In hydrographic and survey applications , one of the key requirements of sonar imaging systems is to deliver absolute georeferenced sonar images and bathymetry map as precisely as possible. The imaging algorithm should also be as efficient as possible and automatic . These considerations have been integrated in the very early stage of the SAMS processing algorithms. In the conventional synthetic aperture sonar imaging scheme , the sonar images are first made in the "slant range plane" focusing at each slant time using beamforming. The image is formed on a relative frame attached to the body frame of the sonar without the need for an absolute positioning system. Then the "temporal" slant image is projected onto the geographical map converting time to range and using the navigation data . However, during projection, interpolation or data fusion may cause some distortions or artifacts in the final map, particularly for high-resolution images.

One of the possible strategies is to directly focus the image on a grid as described on ref. [8][9] . But three points must be addressed here:

- If the grid is defined in a locally referenced frame, a projection step is still needed to further project the image onto the absolutely referenced one . The term "local" means that the projection parameter of the local reference frame will be valid only on some restricted area. For longer surveys , it becomes necessary to adapt the local reference frame parameters.

- The navigation system should deliver precise and robust positioning data. Any artefacts such as jumps must be filtered prior to reconstruction.

- Even if the navigation system delivers very accurate positioning, in coherent SAS, some autofocus method must be used to compensate from residual error .

In the SAMS imaging algorithm , these three points have been carefully taken into account : the sonar images are directly focused on the **absolute** georeferenced frame, the navigation data are filtered, and the phase residual error are corrected. The SAS images and Digital Terrain Model (DTM) are constructed on a ping-to-ping basis meaning that the images are updated in real-time at each ping. This is described in the following section.

B. Synthetic aperture processing on an absolute georeferenced frame

1) Navigation Filtering

In underwater navigation , the AUV is positioned with an inertial navigation system (INS) coupled with a Doppler Velocity log (DVL) and a pressure sensor . The absolute positioning is given by an Ultra or Short Base Line (SUSBL, USBL) installed at the surface , connected to a GPS which interrogates the pinger installed on the AUV. The INS position is updated through a Kalman filter which makes the filtering and fusion of all the auxiliary data and delivers the best 3D positioning solution of the AUV. When the INS receives a new fix position from the USBL, a small jump in the navigation solution will occur (Fig. 4) . This small jump is filtered using the second trajectory computed by integrating platform speed measured by the INS , here designated as the "VI" (integrated speed) trajectory . This trajectory is not affected by the fix update (Fig. 4 left).
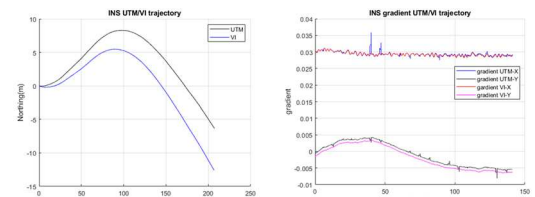

Fig. 4. INS trajectory and gradient

By computing the rigid transform in between the two trajectories , UTM and VI, we obtain the UTM filtered trajectory shown in Fig. 5 .
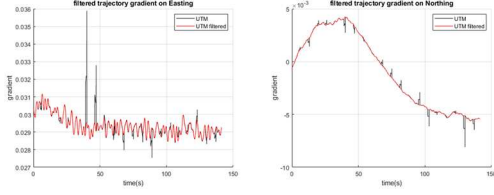
Fig. 5. : Filtered trajectory

Fig. 6. : SAMS incoherent processing

2) Convergence angle and scale factor

When we focus the signal on the UTM (or any other transform) map , we need to compute the true north angle and the true distance in between the Emitter/Receiver position and the pixel position. The true heading is equal to the map heading plus the convergence angle . The true distance is obtained from the distance computed on the map as follow:

$$d_{true} = \sqrt{\gamma^2(d_{map}^2 - depth^2) + depth^2} \qquad (7)$$

where γ is the horizontal scale factor . γ is the product of two factors : the horizontal scale factor due to the geographic transform at depth=0 and the horizontal scale factor due to the sonar depth.

Since the convergence angle and scale factor vary (slowly) with the latitude/longitude and depth of the sonar , their values are updated continuously.

C. SAMS processing algorithms

The SAS imaging algorithms are gathered in a standalone multiplatform library which uses GPU acceleration for faster processing. The images are computed on a ping-to-ping basis : for each emission , the two complex ping images, one or the lower and one for the upper antenna , are computed.

1) Incoherent SAS Imaging

To reconstruct the image mosaic, the amplitude of the signals is averaged for each pixel over successive pings. Working on a georeferenced grid, the pixels altitude needs to be set. The default pixel altitude used is given by a DVL (Doppler Velocity Log) or extracted through the sonar waterfall image itself assuming a flat seabed, but the algorithm can also take into account a pixel depth read from an external bathymetry map or obtained by interferometry between the lower and upper antennas. The synoptic of the algorithm ies detailed on Fig. 6.

2) Incoherent Interferometry

At each ping , the algorithm computes for each insonified pixel the phase difference between the two beamformed complex images of the upper and lower antennas. The situation is described in Fig. 7.
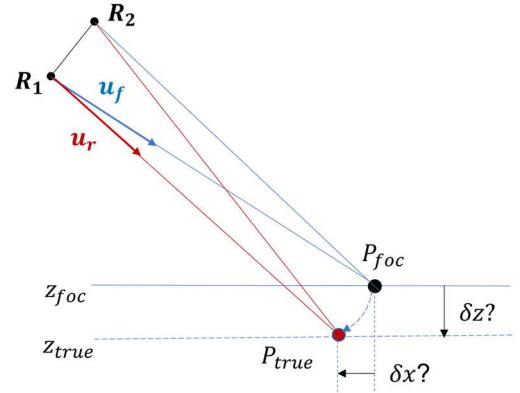
Fig. 7. : Interferometric Phase after focalization at pixel P_{foc}

Assuming an initial 3D pixel position $\textbf{\textit{P}}_{\textbf{foc}}$ (x_{foc},y_{foc},z_{foc}) at range R, when focusing at $\textbf{\textit{P}}_{\textbf{foc}}$ on the upper and lower antenna, we are effectively imaging the true point of focalization $\textbf{P}_{\textbf{true}}$. If the initial pixel altitude is not exact , the measured phase difference is not null : it is the difference between the interferometric phase corresponding to the assumed pixel position $\textbf{\textit{P}}_{\textbf{foc}}$ and the interferometric phase of the effective pixel position $\textbf{P}_{\textbf{true}}$:

$$\Delta\phi_{measured}(\textbf{\textit{P}}_{\textbf{\textit{foc}}}) = \phi_{inter}(\textbf{\textit{P}}_{\textbf{\textit{foc}}}) - \phi_{inter}(\textbf{\textit{P}}_{\textbf{\textit{true}}}) \,(8)$$

with

$$\phi_{inter}(\textbf{\textit{P}}) = 2\pi(R_2 P - R_1 P)/\lambda$$

which can be simplified to

$$\Delta\phi_{measured}(\textbf{\textit{P}}_{\textbf{\textit{foc}}}) \sim (\tfrac{2\pi}{\lambda})\textbf{R}_1\textbf{R}_2 \cdot (\textbf{\textit{u}}_{\textbf{\textit{t}}} - \textbf{\textit{u}}_{\textbf{\textit{foc}}}) \qquad (9)$$

The second equation is given by the direction of focalization which is common to $\mathbf{P_{true}}$ and $\mathbf{P_{foc}}$.

If we note $\mathbf{w}$ the direction of the antenna, we have the relation :

$$w.u_t = w.uf \qquad (10)$$

And since the two points are at the same range we also have as the third equation :

$$R_1 P_{true} = R \qquad (11)$$

The equations 9, 10 and 11 allow to compute exact pixel position $\mathbf{P_{true}}$.

But since we would like to have the sounding at the original pixel location (x_{foc},y_{foc}), we iterate the process with the new starting 3D position x_{foc}, y_{foc},z_{true}.   The iterative procedure is convergent, and, in a few iterations, the true sounding depth is obtained at x_{foc}, y_{foc} position

Note : Equation (10) shows that the shift direction $u_t - uf$, is always orthogonal to the antenna direction (cylindrical symmetry) . It means that if the sonar is travelling on a straight line the shifted focus point is a fixed point and the focalization is perfect as for the "slant range" processing.

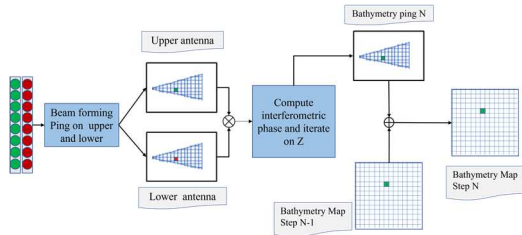The synoptic of the algorithm is detailed on Fig. 8

Fig. 8. : SAMS incoherent interferometry processing

3) Coherent SAS imaging

The coherent processing is also done on a ping-to-ping basis. To build the coherent synthetic aperture over successive ping we need to compensate some residual phase error due to multiple factors mainly   navigation and calibration uncertainty, environmental variability. This is done by using some autofocus technique either at the sensor level or at the pixel level.   At sensor level , the cross-correlation on redundant phase centers will give the correcting phase term[5][6]. At the pixel level, the phase error is estimated on a small region around each pixel. By default, this later method is used and has been implemented in a very efficient manner in the GPU. Fig 9. gives the structure of the processing
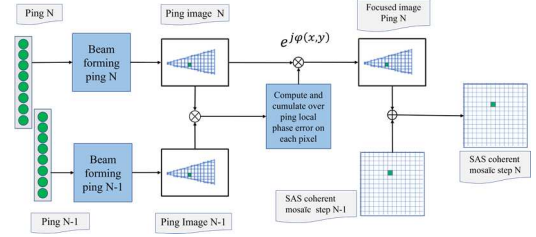
Fig. 9. : SAMS coherent processing

4) Coherent SAS bathymetry

For coherent SAS bathymetry , the two SAS complex images are computed on the upper and lower antennas of the interferometric array. From the phase difference for each pixel, we obtain the sounding depth using the same formula as for the incoherent case.

IV. SAMS150 INTEGRATION AND RESULTS

A. Integration

Data acquisition and processing softwares are integrated in the DelphSuite/DelphSAS software commercialized by Exail (Fig. 10) . The acquisition controller (the embedded software) enables to configure the sonar system : including range selection, pulse type selection, power communication and storage settings. It also records and/or sends the raw sonar and INS data through an ethernet link. In towed fish mode ,when the raw data are sent through ethernet link, the topside software computes and displays the sidescan image and interferometric waterfalls in real-time as a first quality control (image on the top right in Fig. 10). In AUV mode , raw data are stored on a hard disk (typically 8TB is need for 72hours recording). The SAS mosaic and bathymetry map are produced during post-processing using the DelphSAS library. The processing time is at least 2-3 time faster than real-time depending on the resolution parameters. The user needs to select the output geographical projection (UTM, TM etc..) , resolution   (downto 3cm) and imaging mode type (either coherent or incoherent). 3D mosaic and bathymetry map are then displayed at high resolution in the 3D GIS of the DelphSuite software.

Fig. 10. : Software integration

B. First sea trail results on board Ulyx AUV

The SAMS150 was installed on the UlyX AUV to be tested during the ULYSS22C mission aboard vessel Europe from November 30, 2022 to December 4,2022. Prior to the sea trials, the system underwent testing in a very shallow water basin located just outside the Ifremer office.   The SAS coherent image and the SAS incoherent interferometry results obtained are shown in Fig. 11 with a full swath of 300m and a grid resolution of 5cm. The processing is fully automatic, and no post-processing corrections were applied .Despite the rough conditions, the system was able to produce high-quality SAS coherent images and bathymetry maps.

Fig. 11. : First SAMS image and bathymetry map in very shallow water basin

We also assessed the quality of the absolute positioning. As an example , Fig. 12 shows two overlapped survey lines in the north-south and east-west directions. The coincidence between the two lines is very good with a shift being inferior to 1m. The full swath is 400 m. On the left , a zoom on the coherent SAS image of the wreck "la Lune"   . The grid resolution is 5cm and the depth is approximately 80 meters.

Fig. 12. : Absolute position test and image "La Lune"

During this first trial, the stability of the UlyX platform was not yet optimized, and pitch variations of more than +/-5° were observed. Despite these rough conditions, the SAMS 150 system was able to produce high-quality mosaic images and bathymetry map. In Fig. 13 , detailed views of features the area near "la Lune" are displayed. The 3D mosaic image is obtained by draping the high resolution coherent SAS image over the SAS interferometry map

Fig. 13. : Coherent mosaic image of features drapped on the interferometric map

V. CONCLUSION AND PERSPECTIVES

The SAMS150 results demonstrate that synthetic aperture imaging is an efficient and robust imaging technique for both AUV and towed fish platforms :   the processing is automatically adjusted to the stability platform and multiple imaging modes such as coherent or incoherent SAS have been implemented. Incoherent SAS produces high SNR images at very high coverage rate while coherent SAS optimizes the tradeoff between coverage rate and resolution. However, there are still some challenges that need to be addressed to meet the requirements of hydrographic and survey applications. Our ongoing priority tasks include industrializing the product and qualifying the SAS interferometric bathymetry reconstruction to international hydrographic standards (IHO) performances and optimizing and automating the algorithms for real-time embedded processing.

REFERENCES

[1] F. Jean, "Shadows, a new synthetic aperture sonar system, by IXSEA SAS," *OCEANS 2006 - Asia Pacific*, Singapore, 2006, pp. 1-5, doi: 10.1109/OCEANSAP.2006.4393858.

[2] D. Charlot, F. Mosca, ,"Side-scan sonar or synthetic aperture sonar : Towards a new sonar Imaging Concept for survey", Hydro International 2018.

[3] R. Edgar Hansen, 'Introduction to Synthetic Aperture Sonar', Sonar Systems. InTech, Sep. 12, 2011. doi: 10.5772/23122

[4] L. Brignone et al,"Validation at sea for ulyx, the latest deep diving AUV for oceanographic research" , submitted to IEEE Oceans 2023

[5] D.Billon (2000): "Interferometric Synthetic Aperture Sonar:Design and Performance Issues",Proc.5th European Conference on Underwater Acoustics, Lyon, France, July 2000.

[6] A. Bellettini and M. A. Pinto, "Theoretical accuracy of synthetic aperture sonar micronavigation using a displaced phase-center antenna," in *IEEE Journal of Oceanic Engineering*, vol. 27, no. 4, pp. 780-789, Oct. 2002, doi: 10.1109/JOE.2002.805096.

[7] P. Alais, P. Cervenka, P. Challande, V. Lesec, "Non coherent synthetic aperture imaging", Acoustical Imaging 24, 1-8, Plenum Press, 1998.

[8] M. Banks "Studies in high resolution synthetic aperture sonar". PhD thesis, University of London, September 2002.

[9] I. D. Gerg *et al*., "GPU Acceleration for Synthetic Aperture Sonar Image Reconstruction," *Global Oceans 2020: Singapore – U.S. Gulf Coast*, Biloxi, MS, USA, 2020, pp. 1-9, doi: 10.1109/IEEECONF38699.2020.9389388.